IAI Journals.ASM.org

The Mucin Muc2 Limits Pathogen Burdens and Epithelial Barrier Dysfunction during *Salmonella enterica* Serovar Typhimurium Colitis

Maryam Zarepour,[a] Kirandeep Bhullar,[a] Marinieve Montero,[a] Caixia Ma,[a] Tina Huang,[a] Anna Velcich,[b] Lijun Xia,[c] Bruce A. Vallance[a]

Department of Pediatrics, Division of Gastroenterology, Child and Family Research Institute, Vancouver, British Columbia, Canada[a]; Department of Oncology, Albert Einstein Cancer Center/Montefiore Medical Center, Bronx, New York, USA[b]; Cardiovascular Biology Research Program, Oklahoma Medical Research Foundation, Oklahoma City, Oklahoma, USA[c]

***Salmonella enterica* serovar Typhimurium is a model organism used to explore the virulence strategies underlying *Salmonella* pathogenesis. Although intestinal mucus is the first line of defense in the intestine, its role in protection against *Salmonella* is still unclear. The intestinal mucus layer is composed primarily of the Muc2 mucin, a heavily O-glycosylated glycoprotein. The core 3-derived O-glycans of Muc2 are synthesized by core 3 β1,3-*N*-acetylglucosaminyltransferase (C3GnT). Mice lacking these glycans still produce Muc2 but display a thinner intestinal mucus barrier. We began our investigations by comparing *Salmonella*-induced colitis and mucus dynamics in *Muc2*-deficient (*Muc2*$^{-/-}$) mice, *C3GnT*$^{-/-}$ mice, and wild-type C57BL/6 (WT) mice. *Salmonella* infection led to increases in luminal Muc2 secretion in WT and *C3GnT*$^{-/-}$ mice. When *Muc2*$^{-/-}$ mice were infected with *Salmonella*, they showed dramatic susceptibility to infection, carrying significantly higher cecal and liver pathogen burdens, and developing significantly higher barrier disruption and higher mortality rates, than WT mice. We found that the exaggerated barrier disruption in infected *Muc2*$^{-/-}$ mice was *invA* dependent. We also tested the susceptibility of *C3GnT*$^{-/-}$ mice and found that they carried pathogen burdens similar to those of WT mice but developed exaggerated barrier disruption. Moreover, we found that *Muc2*$^{-/-}$ mice were impaired in intestinal alkaline phosphatase (IAP) expression and lipopolysaccharide (LPS) detoxification activity in their ceca, potentially explaining their high mortality rates during infection. Our data suggest that the intestinal mucus layer (Muc2) and core 3 O-glycosylation play critical roles in controlling *Salmonella* intestinal burdens and intestinal epithelial barrier function, respectively.**

Salmonella enterica subspecies 1 serovar Typhimurium is a Gram-negative enteric bacterial pathogen that is a leading clinical cause of food-borne and waterborne diarrheal disease (1). An intracellular pathogen, *S.* Typhimurium is known to use virulence factors encoded on *Salmonella* pathogenicity island 1 (SPI-1), such as *invA*, to infect and/or translocate across the epithelial cells that line the luminal surface of the mammalian intestine. This virulence strategy has been studied extensively *in vitro* and is also known to be involved in the ability of *S.* Typhimurium to cause both mucosal inflammation and diarrhea in infected hosts (2, 3). Despite our detailed understanding of this aspect of *S.* Typhimurium pathogenesis, much less is known about how orally delivered *S.* Typhimurium circumvents the various luminal defenses and intestinal barriers that protect the targeted epithelium, such as the overlying mucus layer.

In large part, the dearth of knowledge in this area reflects the inability of oral *S.* Typhimurium infection of mice to provide a relevant model for the enterocolitis caused by *Salmonella* species (4). Despite the rapid invasion of intestinal epithelial cells in tissue culture by *S.* Typhimurium, very few orally gavaged *S.* Typhimurium bacteria are found to directly infect the intestinal epithelium *in vivo*, resulting in minimal intestinal inflammation. Recently, recognition that the resistance of mice to oral *S.* Typhimurium infection might reflect commensal-microbe-based colonization resistance led to testing of the impact of antibiotic pretreatment. Prior exposure to the antibiotic streptomycin was found to remove competing commensal microbes within mice, facilitating heavy *S.* Typhimurium colonization of the murine large bowel, leading to increased contact with the intestinal epithelium and dramatic cecal and colonic inflammation (5). However, the two mouse strains most commonly used for the *Salmonella* enterocolitis model (C57/BL6 and BALB/c) are known to possess a mutation in their *nramp1* genes, leaving these mice highly susceptible to *S.* Typhimurium and succumbing rapidly to infection (6). To circumvent this limitation, we have recently described a model using the attenuated *S.* Typhimurium Δ*aroA* mutant strain, which still causes severe colitis but typically causes no mortality, even in highly susceptible mouse strains (7). Most studies employing the enterocolitis model have focused on dissecting the virulence strategies of *S.* Typhimurium or exploring the specific host factors that drive the resulting inflammation. In contrast, studies have yet to address how *S.* Typhimurium interacts with, and ultimately crosses, the intestinal mucus layer to reach the underlying epithelium. The mucus barrier is formed predominantly by Muc2, a prominent secretory mucin that overlies the intestinal epithelium. Produced within specialized goblet cells, Muc2 possesses a protein core that is heavily O-glycosylated, with its numerous carbohydrate chains making up 80% of its mass (8). In large part, the function of Muc2 depends on its glycosylation patterns (9, 10, 11). Among the most abundant of these oligosaccharides are the core

Received 11 July 2013 **Accepted** 12 July 2013
Published ahead of print 22 July 2013
Editor: A. J. Bäumler
Address correspondence to Bruce A. Vallance, bvallance@cw.bc.ca.
M.Z. and K.B. are co-first authors.
Supplemental material for this article may be found at http://dx.doi.org/10.1128/IAI.00854-13.

doi:10.1128/IAI.00854-13

3-derived O-glycans, which are synthesized by β1,3-*N*-acetylglucosaminyltransferase (C3GnT) (12). While loss of C3GnT does not prevent Muc2 from forming the mucus layer, *C3GnT*-deficient ($C3GnT^{-/-}$) mice produce a thinner mucus layer than normal, leaving them more susceptible to chemically induced forms of colitis (13).

Once secreted by goblet cells, Muc2 undergoes rapid and dramatic expansion, forming a gel-like layer on the intestinal epithelial surface. This insoluble layer provides a physical barrier that appears to protect the underlying epithelium from direct contact with commensal microbes as well as from many pathogenic insults (14). In addition to secreted mucins, the mucus barrier also contains carbohydrates, antimicrobial peptides, immunoglobulins, electrolytes, lipids, and other intestinal proteins, making it a complex biochemical matrix acting as an important host defense barrier. Recently, intestinal alkaline phosphatase (IAP), a brush border enzyme expressed on the apical sides of enterocytes (and thus at the base of the mucus layer), has emerged as an important gut mucosal defense factor due to its ability to detoxify bacterial lipopolysaccharide (LPS) by removing the phosphate group from LPS and limiting LPS-mediated activation of the innate immune receptor Toll-like receptor 4 (TLR4). Furthermore, IAP-mediated LPS detoxification plays a role in preventing systemic translocation of LPS across the intestinal barrier (15–21). In the absence of this detoxification, systemic translocation of LPS triggers exaggerated inflammatory responses that can ultimately prove fatal to the host through proinflammatory cytokine-induced septic shock (22, 23, 24).

The mucus barrier provides partial protection against several enteric bacterial pathogens, including *Yersinia enterocolitica*, *Shigella flexneri*, and *Citrobacter rodentium* (25, 26, 27). Despite this protection, these and other microbes do ultimately cross the mucus barrier and infect the underlying epithelial cells, raising the questions of how this subversion occurs and whether bacterial pathogens ultimately use the mucus layer as part of their pathogenic strategies. To better define *S.* Typhimurium interactions with the intestinal mucus layer, we infected $Muc2^{-/-}$ and $C3GnT^{-/-}$ mice with Δ*aroA S.* Typhimurium. We found that Muc2 plays an important role in limiting the extent of *Salmonella* colonization of the intestinal lumen, the subsequent mortality of infected hosts, the interactions of *S.* Typhimurium with the intestinal epithelium, and its translocation across the intestinal epithelium. Furthermore, $Muc2^{-/-}$ mice had less IAP expression and significantly less LPS detoxification activity in their cecal tissues than WT mice. We suggest that LPS-triggered inflammatory responses at systemic sites, such as the liver, could be a potential basis for the increased mortality seen in $Muc2^{-/-}$ mice. We noted that lack of core 3 O-glycosylation ($C3GnT^{-/-}$ mice) did not impact the pathogen burdens but resulted in epithelial barrier dysfunction, whereas lack of the entire mucus layer ($Muc2^{-/-}$ mice) caused increased epithelial barrier dysfunction as well as heavier colonization. We also found that in the absence of the mucus layer, as seen in $Muc2^{-/-}$ mice, the barrier dysfunction was dramatically more *invA* dependent than in WT mice. Our study thus demonstrates not only the protective nature of intestinal mucus but also surprising interactions with *S.* Typhimurium that have an impact on its virulence characteristics.

MATERIALS AND METHODS

Mice. C57BL/6 mice were purchased from the Centre for Disease Modeling (CDM) Facility (University of British Columbia), while $Muc2^{-/-}$ and $C3GnT^{-/-}$ mice (on the C57BL/6 background) were bred in our animal facility. Mice were kept in sterilized, filter-topped cages, handled in tissue culture hoods, and fed autoclaved food and water under specific-pathogen-free conditions. The protocols used in the study were approved by the University of British Columbia's Animal Care Committee and were in direct accordance with guidelines provided by the Canadian Council on the Use of Laboratory Animals.

Bacterial strains and infection of mice. The *S.* Typhimurium wild-type (WT) strain SL1344, the SL1344 Δ*invA* strain, and the SL1344 Δ*aroA* strain (6, 28, 29) were grown, with shaking (200 rpm), at 37°C in Luria-Bertani (LB) broth supplemented with 100 μg/ml streptomycin. Approximately 24 h prior to infection, 6- to 8-week-old mice were treated with 20 mg of streptomycin by oral gavage. After streptomycin treatment, mice were infected with the strains mentioned above at a dose of 3×10^7 CFU in 100 μl of phosphate-buffered saline (PBS; pH 7.2) by oral gavage.

Tissue collection and histology. Infected mice were anesthetized using isoflurane and were euthanized by cervical dislocation. For bacterial enumeration, tissues (cecum, liver, spleen, mesenteric lymph nodes [MLN]) and luminal contents were collected in 1 ml of sterile PBS, stored on ice, and homogenized with a Mixer Mill 301 homogenizer (Retsch, Newtown, PA). CFU counts were determined by serial 6-fold dilution of homogenized tissues that had been plated onto LB agar plates supplemented with 100 μg/ml streptomycin and incubated overnight at 37°C. Colony counts were normalized to the weight of the tissue to obtain CFU/g. For histology, cecal tissues were fixed in 10% neutral buffered formalin (Fisher Scientific) overnight and were then transferred to 70% ethanol. Fixed tissues were embedded in paraffin and were cut into 5-μm sections. Tissues were stained with hematoxylin-eosin (H&E) according to standard techniques by the University of British Columbia Histology Laboratory (Vancouver, BC, Canada). To preserve the mucus layer, sections of cecal tissue were fixed in water-free ethanol-Carnoy's fixative (60% ethanol, 30% chloroform, and 10% acetic acid) (all reagents were purchased from Fisher Scientific), and after 3 h of storage at 4°C, samples were transferred to 100% ethanol for subsequent processing. Fixed tissues were embedded in paraffin and were cut into 5-μm sections.

Tissue pathology scoring. The extent of tissue pathology in cecal tissues from uninfected and infected mice was scored using hematoxylin-eosin-stained sections, as described previously (5). Briefly, two observers blinded to the experimental conditions scored cecal tissues for mucosal pathology, including polymorphonuclear leukocyte (PMN) infiltration (scores 0 to 4), goblet cell numbers/depletion (scores 0 to 3), epithelial integrity (scores 0 to 3), and submucosal edema (scores 0 to 3), as outlined previously (2). PMN infiltration was scored at a magnification of ×400 (10 high-power fields), and the average number of cells per high-power field was calculated. Scores were defined, as described previously (5, 7), as follows: 0, <5 cells/high-power field; 1, 5 to 20 cells/high-power field; 2, 21 to 60 cells/high-power field; 3, 61 to 100 cells/high-power field; 4, >100 cells/high-power field.

Immunohistochemistry. For immunohistochemical detection, sections fixed with Carnoy's fixative (for Muc2 and IAP staining) and formalin-fixed sections (for LPS staining) were deparaffinized and boiled for 20 min in citrate buffer (10 mM sodium citrate, 0.05% Tween 20 [pH 6.0]) for antigen retrieval. The sections were then blocked for 20 min using blocking buffer (2% goat serum, 1% bovine serum albumin [BSA], 0.1% Triton X-100, 0.05% Tween 20 in 0.1 M PBS [pH 7.2]) to prevent nonspecific antibody binding. Sections were incubated overnight at 4°C with rabbit anti-Muc2 (dilution, 1:200; Santa Cruz Biotechnology), an anti-LPS antibody (1:50; *Salmonella* O antisera; BD Biosciences), or a rabbit anti-IAP antibody (1:200; Abcam). Alexa Fluor 568-conjugated goat anti-rabbit IgG and Alexa Fluor 488-conjugated goat anti-rabbit IgG (both from Molecular Probes) were used as secondary antibodies at a dilution of 1:2,000. Tissues were mounted using ProLong Gold Antifade reagent

(Molecular Probes) containing 4′,6-diamidino-2-phenylindole (DAPI) for DNA staining. Images were captured using a Zeiss Axio Imager microscope equipped with an AxioCam HRm camera operating through AxioVision software.

***In vivo* intestinal permeability.** As described previously (27), mice used in the study were administered 150 μl of 80-mg/ml FITC (fluorescein isothiocyanate)-dextran (Sigma-Aldrich) by oral gavage. Mice were anesthetized using isoflurane, and blood samples were collected using cardiac puncture. The collected samples were immediately transferred to 3% acid-citrate-dextrose (ACD) containing 20 mM citric acid, 110 nM sodium citrate, 5 mM dextrose (protocol provided by Harald Schulze, Shivdasani laboratory, Dana-Farber Cancer Institute [DFCI]). The concentration of FITC-dextran in serum was measured using a fluorometer (PerkinElmer Life Sciences) (excitation wavelength, 490 nm; emission wavelength, 530 nm).

RNA extraction and quantitative RT-PCR. Cecal tissues stored in RNAlater (Qiagen) at −80°C were thawed on ice, and total RNA was extracted using a Qiagen RNeasy kit as per the manufacturer's instructions. Total RNA was quantified using a NanoDrop spectrophotometer (ND1000). One microgram of RNA was reverse transcribed using an Omniscript reverse transcription (RT) kit (Qiagen). For quantitative PCR, cDNA was diluted 1:5 in RNase- and DNase-free water, and 5 μl of diluted cDNA was added to a PCR mixture (10 μl of Bio-Rad SYBR green supermix, primers at a final concentration of 300 nM; final reaction volume, 20 μl). 18S rRNA was used as a housekeeping gene. Quantitative PCR was carried out using a Bio-Rad MiniOpticon or Opticon 2 system. The sequences for the primers used in this study are as follows: Muc2 forward, 5′ CTGACCAAGAGCGAACACAA 3′; Muc2 reverse, 5′ CATG ACTGGAAGCAACTGGA 3′; IL-6 forward, 5′ GAGGATACCACTCCCA ACAGACC 3′; IL-6 reverse, 5′ AAGTGCATCATCGTTGTTCAT 3′; TNF-α forward, 5′ CATCTTCTCAAAATTCGAGTGACAA 3′; TNF-α reverse, 5′ TGGGAGTAGACAAGGTACAACCC 3′; IL-1β forward, 5′ CAGGATGAGGACATGAGCACC 3′; IL-1β reverse, 5′ CTCTGCAGAC TCAAACTCCAC 3′.

The PCR cycling conditions used were as follows: denaturation at 94°C for 30 s, annealing for 30 s at 55°C for the Muc2 and tumor necrosis factor alpha (TNF-α) genes and at 60°C for the interleukin-6 (IL-6) and IL-1β genes, and extension at 72°C for 45 s, for a total of 30 cycles. There was an initial denaturation step at 95°C for 5 min before PCR cycling, and there was an extension step of 72°C for 10 min after the final cycle. Data were analyzed using Gene Expression Macro OM 3.0 software (Bio-Rad).

LPS dephosphorylation activity analysis. As described previously (18, 24), to assess crude LPS detoxification activity, cecal tissues were homogenized in 500 μl of homogenization buffer, followed by the addition of 5 μl of phenylmethylsulfonyl fluoride (PMSF), a protease inhibitor. Homogenates were centrifuged at 13,200 rpm (4°C for 15 min) to remove the insoluble contents. Bradford analysis was conducted according to the manufacturer's instructions to determine the protein concentrations in the lysates. Eighty microliters of the lysate was incubated with 30 μl of 2.5-mg/ml *Escherichia coli* 055:B5 LPS (L2880; Sigma) or *Salmonella enterica* serotype Typhimurium LPS (L6511; Sigma) at room temperature for 2 h. A malachite green solution was prepared as described previously (30). Forty microliters of the malachite green solution was added to the reaction mixture, which was then incubated for 10 min. The plates were read at an absorbance of 595 nm, and data were analyzed using Microsoft Excel.

Statistical analysis. All the results shown in this study are plotted as mean values with standard errors of the means (SEM). Statistical analysis was performed with GraphPad Prism, version 4.00 for Windows (GraphPad Software, San Diego, CA, USA), using nonparametric Mann-Whitney *t* tests. A *P* value of ≤0.05 was indicative of statistical significance.

RESULTS

***S.* Typhimurium infection of WT mice alters expression of intestinal glycans and the major secretory mucin Muc2.** To investigate intestinal mucin dynamics and glycosylation patterns over the course of *S.* Typhimurium infection, we infected wild-type (WT) mice with Δ*aroA S.* Typhimurium, since we have shown previously that this strain of *S.* Typhimurium causes significant colitis but does not kill even susceptible murine hosts (7). We collected cecal tissues over a 7-day time course and stained them with periodic acid–Schiff's reagent (PAS) as well as with alcian blue. PAS stains neutral carbohydrates (pink/magenta), whereas alcian blue stains acidic carbohydrates (deep blue), while tissues containing both acidic and neutral mucins stain dark blue/purple (31). Assessment of uninfected tissues identified distinct pink staining (neutral carbohydrates) on the epithelial surface (presumably secreted mucins) and blue staining (acidic carbohydrates) within the goblet cells. In contrast, cecal tissues collected at day 3 postinfection (3 dpi) and 7 dpi revealed significant changes in mucin staining, with dark blue/purple coloration throughout the tissues, indicative of changes in the distribution and expression pattern of neutral and acidic mucins during *Salmonella* infection. Specifically on 3 dpi, we noted an increase in PAS/alcian blue staining in goblet cells as well as within the cecal lumen, suggesting that mucin levels were both increased in tissues and secreted into the cecal lumen. Interestingly, by 7 dpi, the PAS/alcian blue staining of goblet cells was dramatically reduced, suggesting that the mucin content within goblet cells was reduced. In contrast, staining of mucus was seen primarily in the cecal lumen, suggesting a relative increase in the proportion of secreted mucins versus mucins contained in goblet cells by this stage of the infection (Fig. 1a).

Since Muc2 is the major secreted mucin within the colon and has been shown previously to protect against enteric bacterial infections (27), we wondered if *Salmonella* infection induced any changes in Muc2 expression. We noted that by 3 dpi, the amount of Muc2 secreted was relatively larger than that for uninfected mice, as assessed by immunostaining. Muc2 was seen on the mucosal surface and within the lumen, and an increase in Muc2 staining intensity inside goblet cells was also noted. On 7 dpi, we found more Muc2 within the cecal lumen (secreted), and more goblet cells within the cecal crypts staining positive for Muc2, than on 3 dpi (Fig. 1b). We also noted a significant increase in the level of *Muc2* gene expression over the course of infection (Fig. 1c). These results suggest that *Salmonella* infection leads to increases in the expression and secretion of Muc2 glycoprotein in WT mice, potentially as a host defense mechanism.

***Muc2*$^{-/-}$ mice display increased susceptibility to *S.* Typhimurium infection.** It has been reported previously that Muc2 plays a protective role against *Citrobacter rodentium* and dextran sulfate sodium (DSS)-induced colitis (27, 32). To assess whether Muc2 protects against *S.* Typhimurium infection, we infected WT and *Muc2*$^{-/-}$ mice with Δ*aroA S.* Typhimurium and compared body weights and survival over the following 9 days. While infected WT mice showed only modest weight loss and ultimately none of the WT mice succumbed to infection, exposure to *S.* Typhimurium was more damaging to *Muc2*$^{-/-}$ mice. Between 6 and 7 dpi, 50% of the *Muc2*$^{-/-}$ mice succumbed to infection, and by 7 dpi, the remaining mice had lost 15 to 20% of their starting body weight and displayed other signs of morbidity, such as hunched posture, inactivity, and piloerection of their fur (Fig. 2). As a result, all the remaining infected *Muc2*$^{-/-}$ mice were euthanized on 7 dpi.

***Muc2*$^{-/-}$ mice carry higher *S.* Typhimurium burdens than WT mice.** Based on the increased Muc2 immunostaining (Fig. 1a)

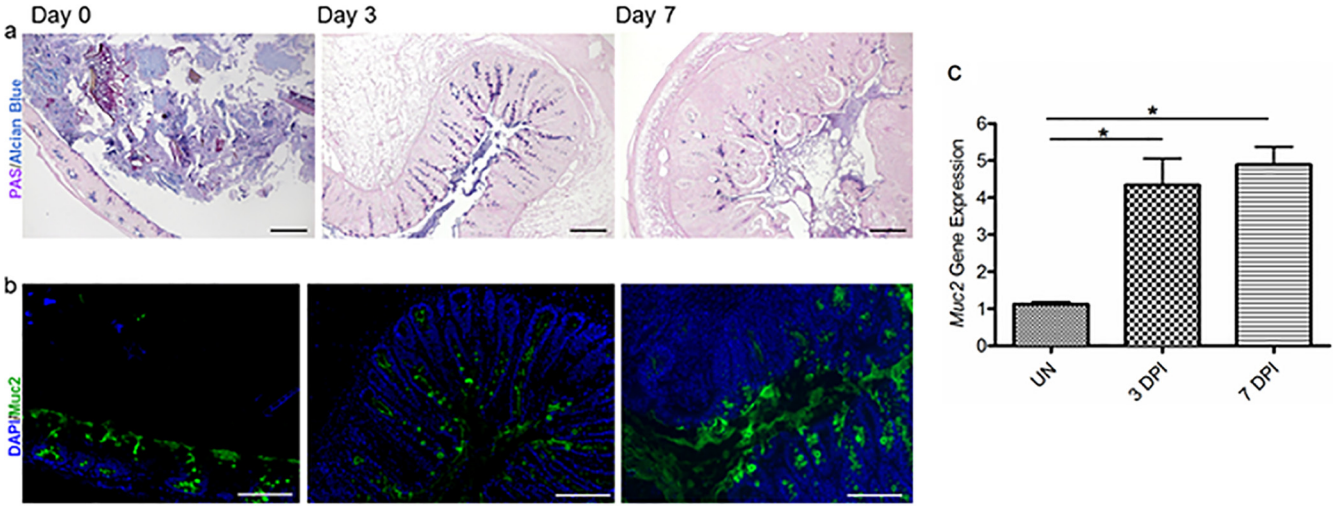

FIG 1 *S.* Typhimurium Δ*aroA* infection results in increased mucin secretion in WT mice. (a) Representative PAS/alcian blue staining of Carnoy's solution-fixed cecal tissues at day 0 (uninfected), 3 dpi, and 7 dpi. Original magnification, ×100; bar, 100 μm. (b) Representative Muc2 immunostaining in the cecum using an anti-Muc2 antibody (green) and a DAPI counterstain (for cellular DNA) (blue) at day 0 (uninfected), 3 dpi, and 7 dpi. Original magnification, ×200; bars, 50 μm. (c) *S.* Typhimurium infection induced significantly higher levels of transcription of the mucin gene *Muc2* in the cecal tissues of WT mice than in uninfected samples. Error bars represent SEM from three independent experiments (9 mice per group). Asterisks indicate significant differences (*, $P < 0.05$) by the Mann-Whitney test.

noted for infected WT mice, we speculated that increased Muc2 secretion during *Salmonella* infection might play a role in controlling pathogenic bacterial burdens. We therefore enumerated the *S.* Typhimurium bacteria within cecal tissues and within the cecal lumen, while also assessing pathogen translocation and/or replication outside the gut, by collecting liver, spleen, and MLN tissues. We observed significantly higher pathogen loads in the ceca of *Muc2*$^{-/-}$ mice than in those of WT mice. Similarly, we recovered higher pathogen burdens from the cecal contents (lumens) of *Muc2*$^{-/-}$ mice than from those of WT mice. We also noted higher pathogen burdens in the livers of *Muc2*$^{-/-}$ mice than in those of WT mice, suggesting that the higher intestinal burden also affected the numbers of microbes reaching (or proliferating within) the liver. In contrast, *S.* Typhimurium was recovered from the spleens and MLN of *Muc2*$^{-/-}$ mice at levels comparable to those for WT mice (Fig. 3), suggesting that *Muc2*$^{-/-}$ mice do not suffer any overt or widespread defects in controlling *S.* Typhimurium burdens at other systemic sites.

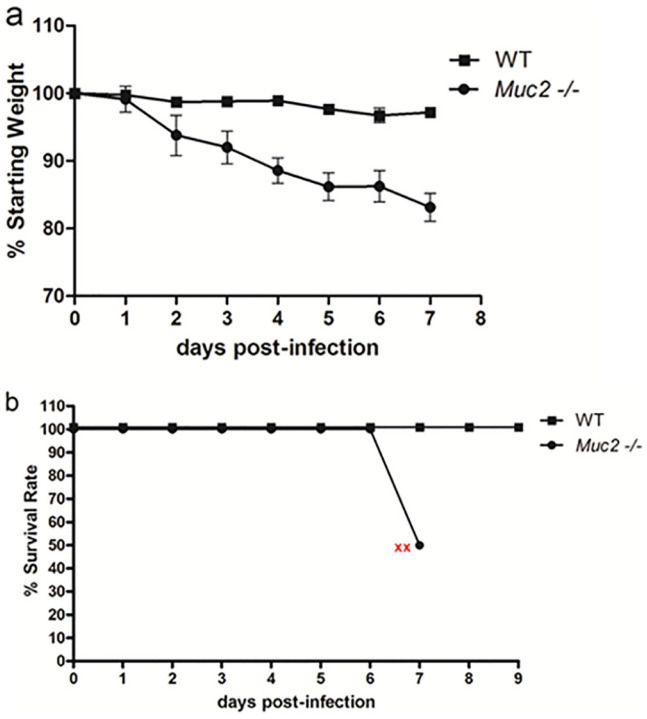

FIG 2 *Muc2*$^{-/-}$ mice exhibit dramatically higher susceptibility to Δ*aroA S.* Typhimurium infection than WT mice. (a) Body weights of WT and *Muc2*$^{-/-}$ mice from 0 to 7 dpi, plotted as percentages of the starting weight. (b) Survival curves of WT and *Muc2*$^{-/-}$ mice following *Salmonella* infection. Red x's indicate the humane endpoint for the remaining *Muc2*$^{-/-}$ mice. Error bars represent SEM from three independent experiments with 9 mice per group.

***Muc2*$^{-/-}$ mice exhibit a level of colitis similar to that for WT mice but suffer exaggerated epithelial barrier disruption.** Next, we sought the cause of the heightened mortality seen in *Salmonella*-infected *Muc2*$^{-/-}$ mice. We undertook histological analysis and pathology scoring to determine whether, in addition to higher pathogen burdens, these mice suffered more-severe tissue damage, potentially explaining their dramatically higher mortality rates. Intestinal pathology was evaluated using previously described histopathological scoring methods (5, 7), and surprisingly, no significant differences in cecal histopathology were observed between infected *Muc2*$^{-/-}$ and WT mice. Histological analysis revealed that *Salmonella* infection elicited pronounced inflammation within the cecal tissues of both WT and *Muc2*$^{-/-}$ mice (Fig. 4a). We observed profound edema and PMN infiltration into the cecal submucosa and mucosa, along with significant damage to epithelial integrity, marked by erosions, crypt loss, and damage to crypt structure, by 3 dpi. This pathology was found to be slightly worse in both mouse strains by 7 dpi, resulting in pathology scores slightly higher than those seen at 3 dpi (Fig. 4b). Since tissue damage was comparable for WT and *Muc2*$^{-/-}$ mice, we next tested whether the lack of mucus led to increased damage

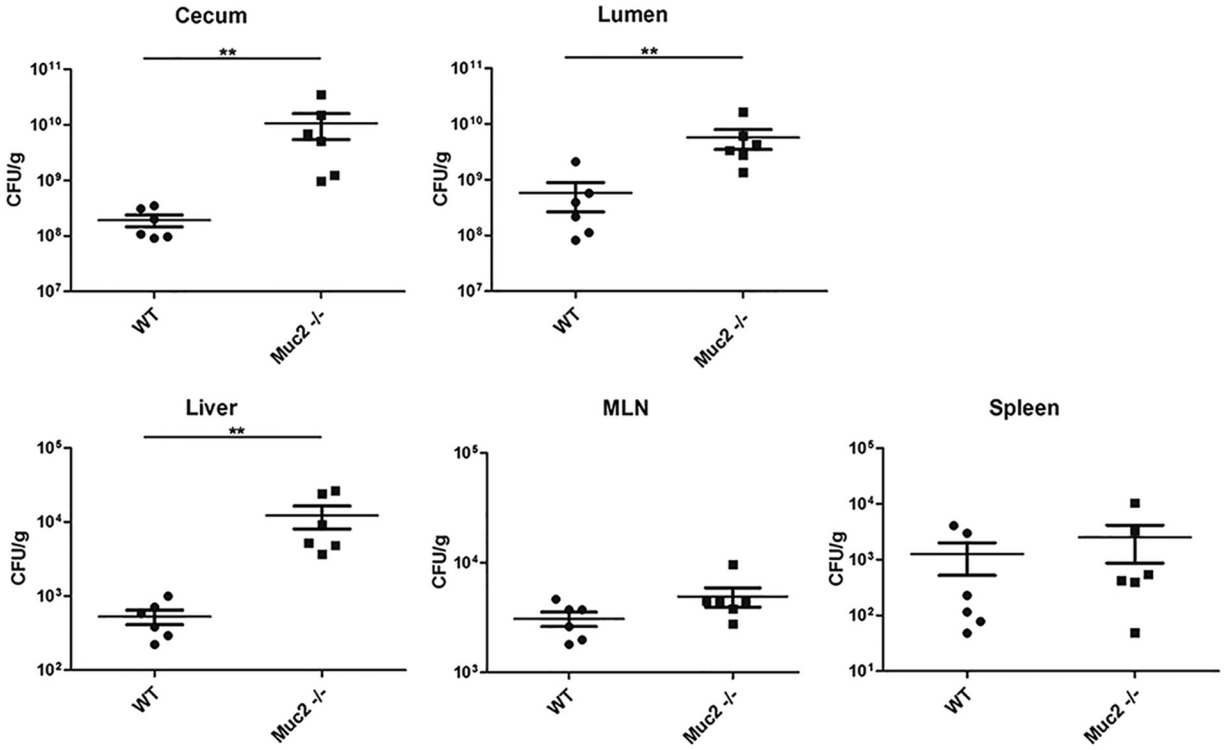

FIG 3 Quantification of Δ*aroA S.* Typhimurium bacteria recovered from the ceca, intestinal lumens, livers, MLN, and spleens of WT and *Muc2*$^{-/-}$ mice. Bacterial burdens carried at 7 dpi in WT and *Muc2*$^{-/-}$ mice are shown. Each data point represents one animal, and the results from 3 independent experiments (9 mice per group) are pooled. Horizontal lines represent means, and error bars represent SEM. Asterisks indicate significant differences (**, $P < 0.01$) by the Mann-Whitney test.

to the intestinal epithelial barrier in *Muc2*$^{-/-}$ mice. Using oral FITC-dextran gavage, we found that the level of FITC-dextran translocation in uninfected *Muc2*$^{-/-}$ mice was modestly, but not significantly, greater than that seen in WT mice. In contrast, while *S.* Typhimurium infection caused no significant impairment of epithelial barrier function in WT mice, infected *Muc2*$^{-/-}$ mice demonstrated significantly greater (3-fold) intestinal permeability ($P < 0.01$) (Fig. 4c).

***S.* Typhimurium-infected *C3GnT*$^{-/-}$ mice show impaired epithelial barrier integrity but bacterial burdens comparable to those of WT mice.** Since Muc2 is a heavily O-glycosylated glycoprotein, we next sought to test whether its critical role in host defense against oral *S.* Typhimurium reflected the Muc2 protein itself or, instead, some aspect of its glycosylation. We therefore infected mice lacking core 3-derived O-glycans (*C3GnT*$^{-/-}$ mice) to determine whether they had a phenotype similar to that of infected *Muc2*$^{-/-}$ mice (i.e., increased pathogen burdens and barrier disruption). Since *C3GnT*$^{-/-}$ mice still produce intestinal mucus, we noted that, like WT mice, they displayed increased accumulation of luminal mucus following infection by *S.* Typhimurium (see Fig. S1 in the supplemental material). Despite this response, we also noted that *Salmonella*-infected *C3GnT*$^{-/-}$ mice showed 8 to 10% greater weight loss than WT mice over the course of infection (Fig. 5a). To address the basis for their increased weight loss, we looked at intestinal and systemic *S.* Typhimurium burdens. Surprisingly, the pathogen burdens for *C3GnT*$^{-/-}$ mice and WT mice were comparable (no statistically significant difference) (Fig. 5c), suggesting that the loss of core 3 O-glycosylation did not significantly affect *Salmonella* colonization. Correspondingly, histological analysis and pathology scoring also failed to reveal any significant differences between *C3GnT*$^{-/-}$ and WT mice (see Fig. S2 in the supplemental material). *Salmonella*-infected *C3GnT*$^{-/-}$ mice displayed levels of infiltrating inflammatory cells, damage to epithelial structure, and submucosal edema similar to those seen in WT mice. Interestingly, *C3GnT*$^{-/-}$ mice did display significantly impaired epithelial integrity relative to that of infected WT mice, as assessed by the FITC-dextran assay (Fig. 5b), suggesting that core 3-derived O-glycans do play a significant role in protecting intestinal barrier function.

The Muc2 layer acts as a physical barrier to limit *Salmonella* contact with the intestinal epithelium. Based on the impact of Muc2 on both *S.* Typhimurium pathogen burdens and the protection of intestinal barrier function, we hypothesized that Muc2 provides a physical barrier to limit *Salmonella* interactions with the underlying epithelium. To investigate the localization of *S.* Typhimurium relative to the mucus layer and epithelium, we fixed tissues with Carnoy's fixative and stained serial sections for Muc2 and *Salmonella* LPS. Immunostaining revealed that in WT mice, the mucus layer provided a distinct barrier, keeping the vast majority of the *S.* Typhimurium bacteria within the cecal lumen and distant from the epithelial surface. In contrast, in *Muc2*$^{-/-}$ mice, *Salmonella* bacteria were seen in close proximity, and even adherent, to the epithelial surface (Fig. 6).

The increased intestinal barrier dysfunction in *S.* Typhimurium-infected *Muc2*$^{-/-}$ mice is *invA* dependent. Cell culture studies have shown previously that *S.* Typhimurium uses *Salmo-*

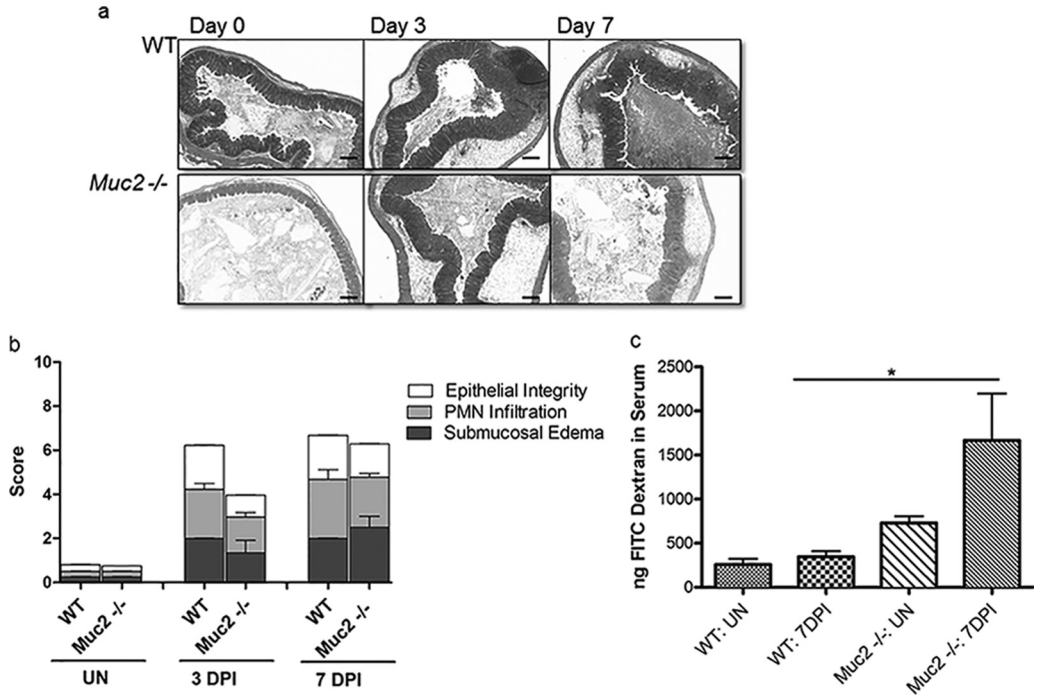

FIG 4 Histology, tissue pathology, and epithelial barrier integrity assessment for Δ*aroA S.* Typhimurium-infected WT and *Muc2*$^{-/-}$ mice. (a) H&E-stained cecal sections (original magnification, ×50; bars, 100 μm) of WT and *Muc2*$^{-/-}$ mice at day 0 (uninfected), 3 dpi, and 7 dpi. (b) Tissue pathology scores. Mucosal pathology scoring includes epithelial barrier integrity, PMN infiltration, and submucosal edema. Each bar represents the average score for 6 to 7 tissues, scored under blinded conditions. (c) FITC-dextran intestinal permeability assay for uninfected (UN) WT and *Muc2*$^{-/-}$ mice and for the same mice at 7 dpi. Bars represent the average values for 9 mice per group, pooled from 3 independent experiments. The asterisk indicates a significant difference (*, $P < 0.05$) by the Mann-Whitney test.

nella pathogenicity island 1 (SPI-1), including InvA, an inner membrane protein component of the SPI-1 type 3 secretion system (T3SS), to infect intestinal epithelial cells and cause barrier disruption (2, 3). Since infected *Muc2*$^{-/-}$ mice suffered from exaggerated barrier disruption, we wondered if this was dependent on the actions of InvA, one of the important proteins involved in *Salmonella* virulence. To test this hypothesis, we first infected WT and *Muc2*$^{-/-}$ mice with wild-type and Δ*invA* (on the wild-type background) strains of *Salmonella* Typhimurium and then euthanized the mice at 3 dpi. Interestingly, wild-type *S.* Typhimurium caused severe cecal pathology and inflammation in both mouse strains, and, as we found with Δ*aroA S.* Typhimurium, *Muc2*$^{-/-}$ mice carried heavier pathogen burdens than WT mice. Moreover, infection caused significant barrier disruption in *Muc2*$^{-/-}$ mice, whereas no disruption was seen in WT mice. When WT mice were infected with Δ*invA Salmonella*, the resulting pathogen burdens in the cecal lumen were similar to those seen with wild-type *Salmonella*, whereas Δ*invA Salmonella* numbers in the cecal tissues, as well as within systemic tissues, were modestly but significantly lower than those of wild-type *Salmonella*. Interestingly, the resulting cecal pathology was only modestly reduced, and no intestinal barrier disruption was noted.

Infected *Muc2*$^{-/-}$ mice were found to carry Δ*invA Salmonella* burdens higher than those of wild-type mice, though significantly lower than wild-type *Salmonella* burdens, in their cecal lumens. The level of pathogen translocation into cecal tissues was dramatically reduced, and *Salmonella* numbers at systemic sites, such as the liver and spleen, were also reduced, to roughly the same degrees as those seen in Δ*invA Salmonella*-infected WT mice. Notably, in contrast to the cecitis suffered by WT mice, no significant cecal pathology was seen in infected *Muc2*$^{-/-}$ mice, and despite their high luminal pathogen burdens, Δ*invA S.* Typhimurium did not cause any barrier disruption (Fig. 7 and 8). Taken together, these findings suggest that although the ability of *S.* Typhimurium to cause cecal pathology in WT mice is partially dependent on *invA*, the dependence on *invA* for inducing cecal pathology is dramatically greater in the absence of a mucus layer (*Muc2*$^{-/-}$ mice), suggesting that the interactions of *Salmonella* with the mucus layer may play a modulatory role in its pathogenesis. Furthermore, while *Muc2*$^{-/-}$ mice infected with wild-type *S.* Typhimurium showed *Salmonella* bacteria in close proximity or adherent to the cecal epithelial surface, mice infected with Δ*invA S.* Typhimurium showed few, if any, of these bacteria adherent to the epithelial surface (see Fig. S3 in the supplemental material). Moreover, *Muc2*$^{-/-}$ mice showed no mortality over the time course of infection with Δ*invA S.* Typhimurium (data not shown), suggesting that pathogen translocation out of the cecum likely plays an important role in the high mortality rates suffered by these mice.

IAP expression and LPS detoxification are impaired in *Muc2*$^{-/-}$ mice. It was surprising that *Muc2*$^{-/-}$ mice succumbed to Δ*aroA S.* Typhimurium, considering that infection by this pathogen is not normally lethal, even to severely immunodeficient mice (7, 33). Considering that their symptoms (hunched appearance, piloerection, and reduced activity) observed during *Salmonella* infection are typically signs of a systemic disease (34), we decided to compare inflammatory responses within the livers of WT and *Muc2*$^{-/-}$ mice. Interestingly, levels of production of the cytokines IL-6, TNF-α, and IL-1β were significantly higher in

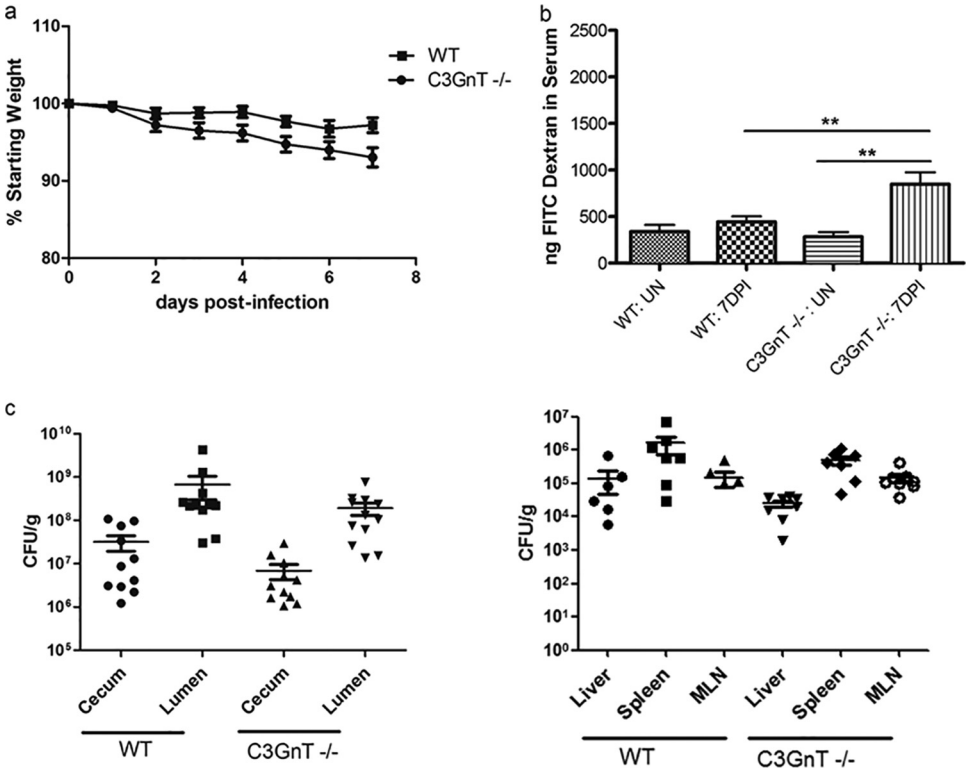

FIG 5 Analysis of the susceptibility of *C3GnT*$^{-/-}$ mice to Δ*aroA S. Typhimurium* infection. (a) Body weights of WT and *C3GnT*$^{-/-}$ mice followed until 7 dpi. (b) FITC-dextran intestinal permeability assay of uninfected (UN) WT and *C3GnT*$^{-/-}$ mice and of the same mice at 7 dpi. Damage to the intestinal barrier was assessed by measuring FITC-dextran in serum, collected by cardiac puncture, 4 h following oral administration. Asterisks indicate significant differences (**, $P < 0.01$) by the Mann-Whitney test. (c) Colonization of *Salmonella*-infected WT and *C3GnT*$^{-/-}$ mice. Each data point represents one animal, and the results from 3 independent experiments (8 to 10 mice per group) are pooled. Horizontal bars represent means; error bars represent SEM.

Muc2$^{-/-}$ mice than in WT mice (see Fig. S4b in the supplemental material), while histologically, the livers of *Muc2*$^{-/-}$ mice displayed much greater signs of inflammation and tissue damage (see Fig. S4a in the supplemental material).

We noted previously that liver injury during *S.* Typhimurium infection is mediated largely by LPS-based activation of the innate receptor TLR4 (35). Interestingly, LPS produced by Gram-negative bacteria within the intestine is typically detoxified by intestinal alkaline phosphatase (IAP), an enzyme expressed by enterocytes (15–20). We therefore wondered if there were any differences in IAP expression or function between WT and *Muc2*$^{-/-}$ mice that could lead to exaggerated inflammatory signaling in response to *S.* Typhimurium bacteria that translocate out of the gut and reach the liver. We found IAP-positive staining on much of the intestinal epithelium of infected WT mice, whereas the staining was comparatively reduced on the epithelial surfaces of *Muc2*$^{-/-}$ mice (Fig. 9). To address whether this reduced staining had any functional impact, we assessed the capacities of cecal tissues from the two mouse strains to detoxify LPS. Strikingly, we identified significantly lower LPS dephosphorylation activity in the cecal tissues of *Muc2*$^{-/-}$ mice than in those of WT mice, suggesting that impaired LPS detoxification could underlie the high mortality rates suffered by infected *Muc2*$^{-/-}$ mice.

DISCUSSION

The intestinal mucus layer is composed predominantly of the secreted mucin Muc2. Synthesized and secreted by goblet cells, Muc2 is a heavily O-glycosylated glycoprotein that forms a gel-like and viscous mesh-like layer overlying the intestinal epithelium. Intestinal mucus is the initial structural barrier encountered by enteric bacterial pathogens and, as such, provides the first line of defense for the host against these and other noxious agents. The presence of the mucus layer has thus necessitated the development of specific virulence strategies allowing enteric pathogens to cross the mucus layer and reach the epithelium, such as flagellum-based motility and even mucus degradation (36). Aside from functioning in host defense, over the course of the evolutionary dialogue between pathogens and the mucus layer, the mucus layer has also been subverted by some microbes to aid in their pathogenesis. For example, mucus can provide attachment sites for pathogenic bacteria (37, 38), as well as providing an energy/food source for adherent bacteria (39, 40). However, despite our growing understanding of the strategies used by enteric pathogens to cross the mucus barrier, it is not entirely clear how they physically interact with the mucus layer.

S. Typhimurium is a leading cause of enterocolitis in humans and is used as a model organism for studying bacterial pathogenesis and host responses to intracellular bacterial infections (1). Pretreatment of mice with streptomycin, followed by infection with *S.* Typhimurium, provides a relevant model for studying *Salmonella*-induced intestinal disease in humans (5). The two most commonly used mouse strains are C57/BL6 and BALB/c, but since these strains suffer from a loss-of-function mutation in their *nramp1* genes, they are extremely susceptible to *Salmonella* infec-

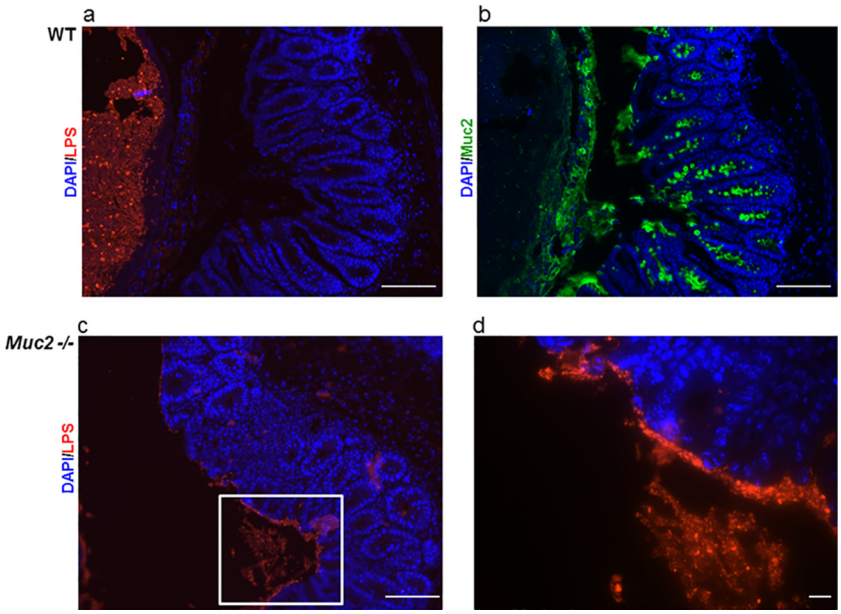

FIG 6 Muc2 provides a physical barrier between the host epithelial surface and *S.* Typhimurium. (a) *Salmonella* LPS staining (red) and DAPI counterstain (blue), showing *Salmonella* bacteria localized to the cecal lumen. (b) Muc2 immunostaining (green) and DAPI counterstain (blue). The thick mucus layer can be seen between the epithelial surface and the lumen. Immunostaining for both markers was done on serial sections of cecal tissue collected from WT mice infected with *Salmonella*. Original magnification, ×200; bars, 50 μm. (c) In contrast to the results for WT mice (panel a), *Salmonella* bacteria can be seen in close proximity to the epithelial surface in the cecal tissues of $Muc2^{-/-}$ mice. Original magnification, ×200; bar, 50 μm. (d) Higher magnification of the inset in panel c. Original magnification, ×630; bar, 5 μm.

tion (6). Recently we have shown the applicability of the attenuated Δ*aroA* strain of *S.* Typhimurium for studying colitis in these mouse strains (7). Our present studies found that Muc2 plays a critical role in host defense against *S.* Typhimurium. $Muc2^{-/-}$ mice showed dramatically heightened susceptibility to *Salmonella* infection compared to that of WT mice, carrying much heavier pathogen burdens both in their intestinal lumens and in mucosal tissues. Our results recall earlier studies with the bacterial pathogen *C. rodentium*, where the loss of Muc2 also led to dramatically heavier intestinal pathogen burdens. In both infection models, the level of Muc2 expression/secretion in WT mice was increased during infection, potentially promoting host defense by removing bacteria from the mucosal surface (27). In $Muc2^{-/-}$ mice, numerous *S.* Typhimurium bacteria were seen in close proximity (or adherent) to the intestinal epithelium, whereas in WT mice, the majority of the *Salmonella* bacteria were segregated from the epithelial surface by the overlying mucus layer, suggesting that aside from the function of mucus as a physical barrier, mucus-mediated flushing can play an important role in controlling pathogen burdens in the gut.

The exaggerated pathogen burdens carried by $Muc2^{-/-}$ mice were accompanied by significant weight loss and other signs of morbidity, requiring the euthanization of all $Muc2^{-/-}$ mice by 7 dpi. This severe response was unexpected, since Δ*aroA S.* Typhimurium typically does not cause serious morbidity or any mortality in other mouse strains, including severely immunodeficient $RAG1^{-/-}$ mice, which can carry very high systemic burdens of this mutant strain (33). We hypothesize, however, that the susceptibility of the $Muc2^{-/-}$ mice to this mutant reflects not only their heavy pathogen burdens but also the exaggerated barrier dysfunction they suffer during infection. A number of studies have shown that *S.* Typhimurium can cause tight-junction disruption in infected epithelial cells, resulting in increased epithelial permeability (41–44). Despite this *in vitro* phenotype, we and others have not been able to detect overt intestinal barrier dysfunction in other mouse strains orally infected by *S.* Typhimurium. The current findings thus indicate that loss of Muc2 leaves the intestinal epithelium unusually susceptible to *S.* Typhimurium-driven barrier disruption.

To better define the mechanisms behind the barrier disruption seen in infected $Muc2^{-/-}$ mice, we infected WT and $Muc2^{-/-}$ mice with a *Salmonella* strain lacking *Salmonella* pathogenicity island 1 (SPI-1)-dependent type III secretion. *invA* is the first gene in the *invABC* operon, is located in SPI-1, and is required, at least *in vitro*, for the invasion of epithelial cells by *S.* Typhimurium (3, 45). When $Muc2^{-/-}$ mice were infected with the Δ*invA* mutant, barrier function was not disrupted, and very minor histological damage was observed. Taken together with the observation that systemic Δ*invA* pathogen burdens were dramatically reduced in $Muc2^{-/-}$ mice, these data suggest that the susceptibility of the $Muc2^{-/-}$ mice was dependent on *invA*. In contrast, the Δ*invA* mutant was still able to cross the intestinal epithelia of WT mice and cause significant cecal pathology, though less than that seen with wild-type *Salmonella*. These results suggest that potential interactions with intestinal mucus provide *Salmonella* (in this case, an *invA* mutant) with increased opportunities for uptake and translocation out of the gut lumen, potentially by dendritic cells or macrophages, through pathogen-driven but non-SPI-1-dependent mechanisms (46, 47). In contrast, in the absence of mucus, SPI-1-dependent mechanisms appear to play a more important role in the crossing of the intestinal epithelial barrier by *Salmonella*. These results suggest that *S.* Typhimurium bacteria adher-

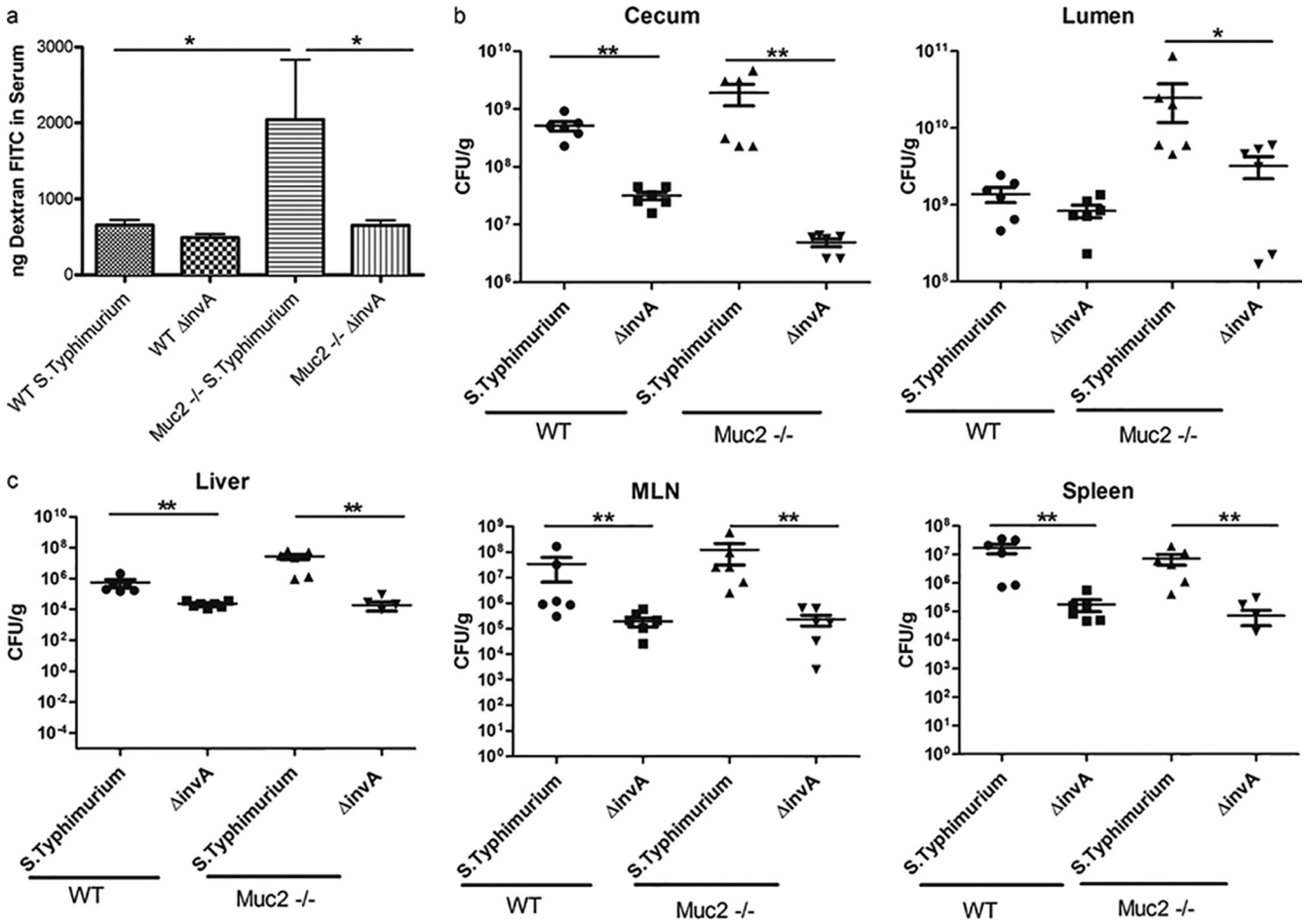

FIG 7 Analysis of *invA*-dependent susceptibility of *Muc2*$^{-/-}$ mice. (a) FITC-dextran intestinal permeability assay for WT mice and *Muc2*$^{-/-}$ mice infected with wild-type *Salmonella* Typhimurium SL1344 and a Δ*invA Salmonella* strain (SL1344 background). (b and c) Colonization of WT and *Muc2*$^{-/-}$ mice after infection with the wild-type or Δ*invA Salmonella* strain is shown for the cecum and lumen (b) and for the liver, spleen, and MLN (c). Horizontal bars represent means; error bars represent SEM. Asterisks indicate significant differences (*, $P < 0.05$; **, $P < 0.01$) by the Mann-Whitney test for 9 mice per group in 3 independent experiments.

ent to the mucosal surface may be expressing the genes involved in the SPI-1 virulence system and that there may be differential expression of this system in *Muc2*$^{-/-}$ mice versus WT mice, dictated by the direct interactions between *Salmonella* bacteria and the epithelial surface. Since in *Muc2*$^{-/-}$ mice infected with the Δ*invA* strain, there is no close adherence to the epithelial surface, the expression of this virulence system may be impaired, thereby reducing the pathology and pathophysiology seen in these mice.

Aside from the mucus layer, there are other factors that determine host susceptibility to an enteric bacterial pathogen, including the enzyme intestinal alkaline phosphatase (IAP). Recently there has been renewed interest in IAP activity and its role in promoting intestinal mucosal defense (15). Several studies have shown that LPS dephosphorylation mediated by IAP protects the host against LPS-induced inflammation as well as reducing the systemic translocation of enteric bacteria (15–24). To investigate whether IAP activity was playing a role in the increased susceptibility/morbidity of *Muc2*$^{-/-}$ mice in our model, we stained for IAP and found that *Muc2*$^{-/-}$ mice had reduced IAP expression as well as reduced LPS dephosphorylation activity (a measure of the activity of IAP) within their cecal tissues. While the basis for this impairment is unclear, a recent study has reported altered expression of other enzymes in the intestinal epithelia of *Muc2*$^{-/-}$ mice (48). However, it is not clear at this point whether these changes in epithelial cell function reflect a direct role for Muc2 mucin or, alternatively, result from increased microbial interactions with the epithelium.

Interestingly, we also noted a dramatic increase in proinflammatory cytokine gene levels within the livers of *Muc2*$^{-/-}$ mice. We speculate that impaired intestinal barrier function in concert with reduced LPS detoxification within the ceca of *Muc2*$^{-/-}$ mice leads to the translocation of *Salmonella* bacteria carrying highly proinflammatory LPS to the liver, resulting in increased inflammation (through TLR4-LPS signaling) and exaggerated damage to the liver, ultimately contributing to the higher mortality observed in these mice. These results are in line with our previous studies showing the importance of TLR4 signaling in mediating inflammatory responses in the liver (35). Our study also sheds light on the complex interactions between host factors (mucus layer, IAP) and pathogen factors (virulence genes) that ultimately determine the outcome of an infection.

To better define how Muc2 plays such a critical role in control-

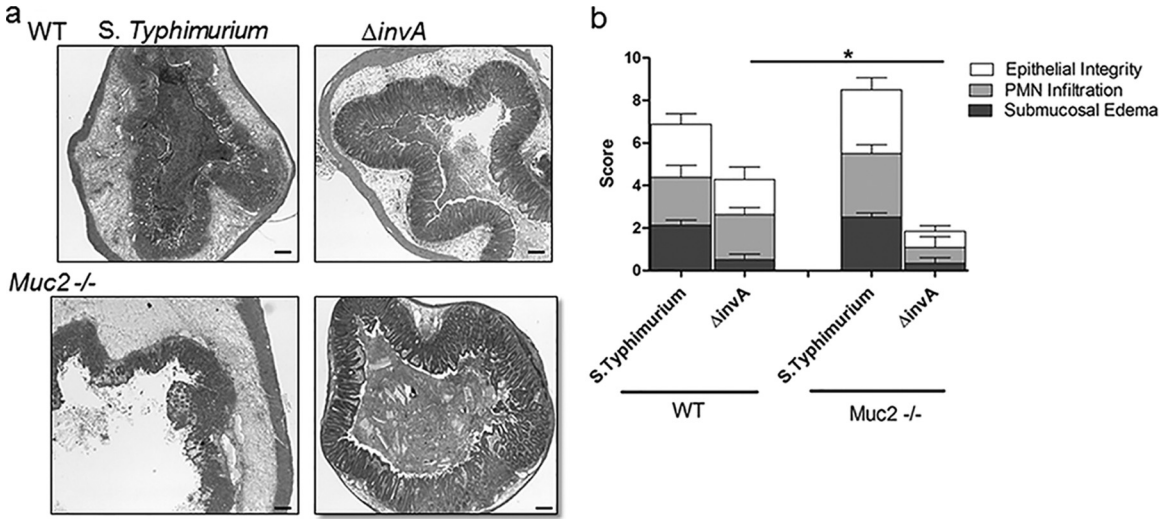

FIG 8 Histological and pathological analyses of WT and *Muc2*$^{-/-}$ mice upon infection with wild-type and Δ*invA Salmonella* strains. (a) Representative H&E-stained images for WT and *Muc2*$^{-/-}$ mice infected with wild-type and Δ*invA Salmonella* strains. Original magnification, ×50; bars, 100 μm. (b) Tissue pathology scores. Pathology scoring included damage to epithelial integrity, PMN infiltration, and submucosal edema. Each bar represents the average for 9 to 10 tissues. The asterisk indicates a significant difference (*, $P < 0.05$) by the Mann-Whitney test.

ling *S.* Typhimurium pathogenesis, we infected mice lacking different components of this glycoprotein. Muc2 is a heavily O-glycosylated mucin, and the impact of its glycosylation was noted by a recent study examining different glycosylation patterns of Muc2 in mice and humans (49, 50). In agreement with previous findings (13), we found that core 3 O-glycosylation plays a major role in protecting intestinal barrier function. Mice lacking core 3-derived O-glycans possess a thinner intestinal mucus layer, and although they do not develop any spontaneous gut diseases, they do show increased susceptibility to DSS-induced colitis (13). Infecting these *C3GnT*$^{-/-}$ mice, we found no significant differences from WT mice in infection-induced histology, pathology, or *S.* Typhi-

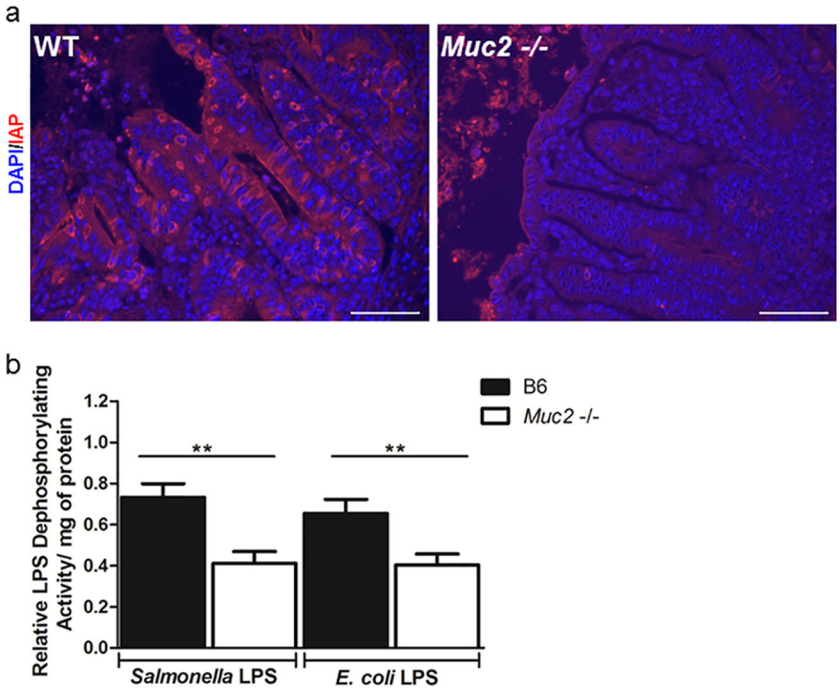

FIG 9 *Muc2*$^{-/-}$ mice are impaired in IAP staining and activity. (a) Representative IAP immunostaining (red) in the ceca of WT and *Muc2*$^{-/-}$ mice at day 7 after infection with Δ*aroA S.* Typhimurium. The DAPI counterstain is shown in blue. Original magnification, ×400; bars, 20 μm. (b) Analysis of *ex vivo* LPS dephosphorylation activity in the cecal tissues of WT and *Muc2*$^{-/-}$ mice infected with Δ*aroA S.* Typhimurium (assessed at 7 dpi). Homogenized cecal tissues were incubated with *Salmonella* LPS or *Escherichia coli* LPS for 2 h, and the malachite green assay was used to measure activity (absorbance at 595 nm). Activity was calculated as relative LPS dephosphorylation activity/mg of protein (normalized to the value for uninfected controls in each group). There were 9 mice per group. Asterisks indicate significant differences (**, $P < 0.01$) by the Mann-Whitney test.

murium burdens. However, these mice still suffered from greater epithelial barrier disruption during infection than WT mice. This suggests that the core 3 glycosylation component of the mucus layer may play a role in controlling *Salmonella*-driven disruption of epithelial barrier integrity, whereas the Muc2 protein and its remaining glycosylation are the key factors in controlling *S.* Typhimurium burdens and overt intestinal pathology.

Increased release of mucus into the intestinal lumen, as seen during *Salmonella* infection in WT and *C3GnT*$^{-/-}$ mice, may help protect the epithelium by limiting pathogen contact and barrier disruption. This may reflect a unique action of secreted mucins, since it has been shown previously that *Muc1*$^{-/-}$ mice were not more susceptible than WT mice to *S.* Typhimurium infection (51), whereas in this study, we show increased susceptibility of *Muc2*$^{-/-}$ mice to *S.* Typhimurium infection. We believe that such a protective role may be a generalized defense against many enteric bacterial pathogens. Indeed, there have been reports of Muc2 interactions with other enteric pathogens, including *Campylobacter jejuni* (52) and the attaching and effacing (A/E) pathogen *Citrobacter rodentium* (53).

There has been growing recognition of the important role played by the mucus barrier in regulating the severity of infectious diseases, but the specifics of how enteric bacterial pathogens interact with mucus and mucus components remain unclear. This study unravels the importance of Muc2, a major secreted mucin, during infection with yet another enteric pathogen, *S.* Typhimurium, and it is the first study to provide insight into the importance of core 3 O-glycosylation during *Salmonella* infection. This study also provides insights into the potential role of mucus in modulating *Salmonella* pathogenesis. Considering that the mucus layer acts as a frontline defense barrier, further investigation of interactions between enteric pathogens and the mucus layer may aid in the development of therapeutic strategies.

ACKNOWLEDGMENTS

We thank Kirk Bergstrom for helpful discussions. We thank Martin Stahl for careful proofreading of the manuscript.

This study was funded by operating grants from the Crohn's and Colitis Foundation of Canada (CCFC) and the Canadian Institutes of Health Research (CIHR) awarded to B.A.V. M.Z. was funded by a Child and Family Research Institute (CFRI) postdoctoral fellowship. K.B. was funded by a CFRI graduate studentship. B.A.V. is the Children with Intestinal and Liver Disorders (CHILD) Foundation Chair in Pediatric IBD Research and the Canada Research Chair in Pediatric Gastroenterology (tier 2).

REFERENCES

1. **Ohl ME, Miller SI.** 2001. *Salmonella*: a model for bacterial pathogenesis. Annu. Rev. Med. **52:**259–274.
2. **Galán JE, Ginocchio C, Costeas P.** 1992. Molecular and functional characterization of the *Salmonella* invasion gene *invA*: homology of InvA to members of a new protein family. J. Bacteriol. **174:**4338–4349.
3. **Galán JE, Curtiss R, III.** 1989. Cloning and molecular characterization of genes whose products allow *Salmonella typhimurium* to penetrate tissue culture cells. Proc. Natl. Acad. Sci. U. S. A. **86:**6383–6387.
4. **Santos RL, Zhang S, Tsolis RM, Kingsley RA, Adams LG, Bäumler AJ.** 2001. Animal models of *Salmonella* infections: enteritis versus typhoid fever. Microbes Infect. **3:**1335–1344.
5. **Barthel M, Hapfelmeier S, Quintanilla-Martínez L, Kremer M, Rohde M, Hogardt M, Pfeffer K, Rüssmann H, Hardt WD.** 2003. Pretreatment of mice with streptomycin provides a *Salmonella enterica* serovar Typhimurium colitis model that allows analysis of both pathogen and host. Infect. Immun. **71:**2839–2858.
6. **Vidal S, Tremblay ML, Govoni G, Gauthier S, Sebastiani G, Malo D, Skamene E, Olivier M, Jothy S, Gros P.** 1995. The Ity/Lsh/Bcg locus: natural resistance to infection with intracellular parasites is abrogated by disruption of the Nramp1 gene. J. Exp. Med. **182:**655–666.
7. **Månsson LE, Montero M, Zarepour M, Bergstrom KS, Ma C, Huang T, Man C, Grassl GA, Vallance BA.** 2012. MyD88 signaling promotes both mucosal homeostatic and fibrotic responses during *Salmonella*-induced colitis. Am. J. Physiol. Gastrointest. Liver Physiol. **303:**G311–G323.
8. **Johansson ME, Larsson JM, Hansson GC.** 2011. The two mucus layers of colon are organized by the MUC2 mucin, whereas the outer layer is a legislator of host-microbial interactions. Proc. Natl. Acad. Sci. U. S. A. **108**(Suppl 1):4659–4665.
9. **Pusztai A, Ewen SW, Grant G, Peumans WJ, Van Damme EJ, Coates ME, Bardocz S.** 1995. Lectins and also bacteria modify the glycosylation of gut surface receptors in the rat. Glycoconj. J. **12:**22–35.
10. **Robbe-Masselot C, Herrmann A, Carlstedt I, Michalski JC, Capon C.** 2008. Glycosylation of the two O-glycosylated domains of human MUC2 mucin in patients transposed with artificial urinary bladders constructed from proximal colonic tissue. Glycoconj. J. **25:**213–224.
11. **Holmén JM, Olson FJ, Karlsson H, Hansson GC.** 2002. Two glycosylation alterations of mouse intestinal mucins due to infection caused by the parasite *Nippostrongylus brasiliensis*. Glycoconj. J. **19:**67–75.
12. **Iwai T, Inaba N, Naundorf A, Zhang Y, Gotoh M, Iwasaki H, Kudo T, Togayachi A, Ishizuka Y, Nakanishi H, Narimatsu H.** 2002. Molecular cloning and characterization of a novel UDP-GlcNAc:GalNAc-peptide β1,3-*N*-acetylglucosaminyltransferase (β3Gn-T6), an enzyme synthesizing the core 3 structure of O-glycans. J. Biol. Chem. **277:**12802–12809.
13. **An G, Wei B, Xia B, McDaniel JM, Ju T, Cummings RD, Braun J, Xia L.** 2007. Increased susceptibility to colitis and colorectal tumors in mice lacking core 3-derived O-glycans. J. Exp. Med. **204:**1417–1429.
14. **Kim YS, Ho SB.** 2010. Intestinal goblet cells and mucins in health and disease: recent insights and progress. Curr. Gastroenterol. Rep. **12:**319–330.
15. **Lallès JP.** 2010. Intestinal alkaline phosphatase: multiple biological roles in maintenance of intestinal homeostasis and modulation by diet. Nutr. Rev. **68:**323–332.
16. **Poelstra K, Bakker WW, Klok PA, Hardonk MJ, Meijer DK.** 1997. A physiologic function for alkaline phosphatase: endotoxin detoxification. Lab. Invest. **76:**319–327.
17. **Poelstra K, Bakker WW, Klok PA, Kamps JA, Hardonk MJ, Meijer DK.** 1997. Dephosphorylation of endotoxin by alkaline phosphatase in vivo. Am. J. Pathol. **151:**1163–1169.
18. **Goldberg RF, Austen WG, Jr, Zhang X, Munene G, Mostafa G, Biswas S, McCormack M, Eberlin KR, Nguyen JT, Tatlidede HS, Warren HS, Narisawa S, Millán JL, Hodin RA.** 2008. Intestinal alkaline phosphatase is a gut mucosal defense factor maintained by enteral nutrition. Proc. Natl. Acad. Sci. U. S. A. **105:**3551–3556.
19. **Bates JM, Akerlund J, Mittge E, Guillemin K.** 2007. Intestinal alkaline phosphatase detoxifies lipopolysaccharide and prevents inflammation in zebrafish in response to the gut microbiota. Cell Host Microbe **2:**371–382.
20. **Beumer C, Wulferink M, Raaben W, Fiechter D, Brands R, Seinen W.** 2003. Calf intestinal alkaline phosphatase, a novel therapeutic drug for lipopolysaccharide (LPS)-mediated diseases, attenuates LPS toxicity in mice and piglets. J. Pharmacol. Exp. Ther. **307:**737–744.
21. **Fukata M, Abreu MT.** 2007. TLR4 signalling in the intestine in health and disease. Biochem. Soc. Trans. **35:**1473–1478.
22. **van Veen SQ, van Vliet AK, Wulferink M, Brands R, Boermeester MA, van Gulik TM.** 2005. Bovine intestinal alkaline phosphatase attenuates the inflammatory response in secondary peritonitis in mice. Infect. Immun. **73:**4309–4314.
23. **Bentala H, Verweij WR, Huizinga-Van der Vlag A, van Loenen-Weemaes AM, Meijer DK, Poelstra K.** 2002. Removal of phosphate from lipid A as a strategy to detoxify lipopolysaccharide. Shock **18:**561–566.
24. **Ghosh S, DeCoffe D, Brown K, Rajendiran E, Estaki M, Dai C, Yip A, Gibson DL.** 2013. Fish oil attenuates omega-6 polyunsaturated fatty acid-induced dysbiosis and infectious colitis but impairs LPS dephosphorylation activity causing sepsis. PLoS One **8:**e55468. doi:10.1371/journal.pone.0055468.
25. **Mantle M, Basaraba L, Peacock SC, Gall DG.** 1989. Binding of *Yersinia enterocolitica* to rabbit intestinal brush border membranes, mucus, and mucin. Infect. Immun. **57:**3292–3299.
26. **Nutten S, Sansonetti P, Huet G, Bourdon-Bisiaux C, Meresse B, Colombel JF, Desreumaux P.** 2002. Epithelial inflammation response in-

duced by *Shigella flexneri* depends on mucin gene expression. Microbes Infect. **4:**1121–1124.
27. **Bergstrom KS, Kissoon-Singh V, Gibson DL, Ma C, Montero M, Sham HP, Ryz N, Huang T, Velcich A, Finlay BB, Chadee K, Vallance BA.** 2010. Muc2 protects against lethal infectious colitis by disassociating pathogenic and commensal bacteria from the colonic mucosa. PLoS Pathog. **6:**e1000902. doi:10.1371/journal.ppat.1000902.
28. **Menendez A, Arena ET, Guttman JA, Thorson L, Vallance BA, Vogl W, Finlay BB.** 2009. *Salmonella* infection of gallbladder epithelial cells drives local inflammation and injury in a model of acute typhoid fever. J. Infect. Dis. **200:**1703–1713.
29. **Chatfield SN, Strahan K, Pickard D, Charles IG, Hormaeche CE, Dougan G.** 1992. Evaluation of *Salmonella typhimurium* strains harbouring defined mutations in *htrA* and *aroA* in the murine salmonellosis model. Microb. Pathog. **12:**145–151.
30. **Baykov AA, Evtushenko OA, Avaeva SM.** 1988. A malachite green procedure for orthophosphate determination and its use in alkaline phosphatase-based enzyme immunoassay. Anal. Biochem. **171:**266–270.
31. **Yamabayashi S.** 1987. Periodic acid-Schiff-alcian blue: a method for the differential staining of glycoproteins. Histochem. J. **19:**565–571.
32. **Van der Sluis M, De Koning BA, De Bruijn AC, Velcich A, Meijerink JP, Van Goudoever JB, Büller HA, Dekker J, Van Seuningen I, Renes IB, Einerhand AW.** 2006. Muc2-deficient mice spontaneously develop colitis, indicating that MUC2 is critical for colonic protection. Gastroenterology **131:**117–129.
33. **Hess J, Ladel C, Miko D, Kaufmann SH.** 1996. *Salmonella typhimurium aroA*$^-$ infection in gene-targeted immunodeficient mice: major role of CD4$^+$ TCR-αβ cells and IFN-γ in bacterial clearance independent of intracellular location. J. Immunol. **156:**3321–3326.
34. **Özkaya H, Akcan AB, Aydemir G, Aydinöz S, Razia Y, Gammon ST, McKinney J.** 2012. *Salmonella typhimurium* infections in BALB/c mice: a comparison of tissue bioluminescence, tissue cultures and mice clinical scores. New Microbiol. **35:**53–59.
35. **Vazquez-Torres A, Vallance BA, Bergman MA, Finlay BB, Cookson BT, Jones-Carson J, Fang FC.** 2004. Toll-like receptor 4 dependence of innate and adaptive immunity to *Salmonella*: importance of the Kupffer cell network. J. Immunol. **172:**6202–6208.
36. **McGuckin MA, Lindén SK, Sutton P, Florin TH.** 2011. Mucin dynamics and enteric pathogens. Nat. Rev. Microbiol. **9:**265–278.
37. **Lillehoj EP, Hyun SW, Kim BT, Zhang XG, Lee DI, Rowland S, Kim KC.** 2001. Muc1 mucins on the cell surface are adhesion sites for *Pseudomonas aeruginosa*. Am. J. Physiol. Lung Cell. Mol. Physiol. **280:**L181–L187.
38. **Rajkumar R, Devaraj H, Niranjali S.** 1998. Binding of *Shigella* to rat and human intestinal mucin. Mol. Cell. Biochem. **178:**261–268.
39. **Aristoteli LP, Willcox MD.** 2003. Mucin degradation mechanisms by distinct *Pseudomonas aeruginosa* isolates in vitro. Infect. Immun. **71:**5565–5575.
40. **Berg RD.** 1996. The indigenous gastrointestinal microflora. Trends Microbiol. **4:**430–435.
41. **Boyle EC, Brown NF, Finlay BB.** 2006. *Salmonella enterica* serovar Typhimurium effectors SopB, SopE, SopE2 and SipA disrupt tight junction structure and function. Cell. Microbiol. **8:**1946–1957.
42. **Finlay BB, Falkow S.** 1990. *Salmonella* interactions with polarized human intestinal Caco-2 epithelial cells. J. Infect. Dis. **162:**1096–1106.
43. **Jepson MA, Collares-Buzato CB, Clark MA, Hirst BH, Simmons NL.** 1995. Rapid disruption of epithelial barrier function by *Salmonella typhimurium* is associated with structural modification of intercellular junctions. Infect. Immun. **63:**356–359.
44. **Jepson MA, Schlecht HB, Collares-Buzato CB.** 2000. Localization of dysfunctional tight junctions in *Salmonella enterica* serovar Typhimurium-infected epithelial layers. Infect. Immun. **68:**7202–7208.
45. **Coombes BK, Coburn BA, Potter AA, Gomis S, Mirakhur K, Li Y, Finlay BB.** 2005. Analysis of the contribution of *Salmonella* pathogenicity islands 1 and 2 to enteric disease progression using a novel bovine ileal loop model and a murine model of infectious enterocolitis. Infect. Immun. **73:**7161–7169.
46. **Yrlid U, Svensson M, Håkansson A, Chambers BJ, Ljunggren HG, Wick MJ.** 2001. In vivo activation of dendritic cells and T cells during *Salmonella enterica* serovar Typhimurium infection. Infect. Immun. **69:**5726–5735.
47. **Kalupahana RS, Mastroeni P, Maskell D, Blacklaws BA.** 2005. Activation of murine dendritic cells and macrophages induced by *Salmonella enterica* serovar Typhimurium. Immunology **115:**462–472.
48. **Yang K, Popova NV, Yang WC, Lozonschi I, Tadesse S, Kent S, Bancroft L, Matise I, Cormier RT, Scherer SJ, Edelmann W, Lipkin M, Augenlicht L, Velcich A.** 2008. Interaction of Muc2 and Apc on Wnt signaling and in intestinal tumorigenesis: potential role of chronic inflammation. Cancer Res. **68:**7313–7322.
49. **Larsson JM, Karlsson H, Crespo JG, Johansson ME, Eklund L, Sjövall H, Hansson GC.** 2011. Altered O-glycosylation profile of MUC2 mucin occurs in active ulcerative colitis and is associated with increased inflammation. Inflamm. Bowel Dis. **17:**2299–2307.
50. **Larsson JM, Karlsson H, Sjövall H, Hansson GC.** 2009. A complex, but uniform O-glycosylation of the human MUC2 mucin from colonic biopsies analyzed by nanoLC/MSn. Glycobiology **19:**756–766.
51. **McAuley JL, Linden SK, Png CW, King RM, Pennington HL, Gendler SJ, Florin TH, Hill GR, Korolik V, McGuckin MA.** 2007. MUC1 cell surface mucin is a critical element of the mucosal barrier to infection. J. Clin. Invest. **117:**2313–2324.
52. **Tu QV, McGuckin MA, Mendz GL.** 2008. *Campylobacter jejuni* response to human mucin MUC2: modulation of colonization and pathogenicity determinants. J. Med. Microbiol. **57:**795–802.
53. **Lindén SK, Florin TH, McGuckin MA.** 2008. Mucin dynamics in intestinal bacterial infection. PLoS One **3:**e3952. doi:10.1371/journal.pone.0003952.